

Daniel G. H. Devos
Philip J. Kilner

Calculations of cardiovascular shunts and regurgitation using magnetic resonance ventricular volume and aortic and pulmonary flow measurements

Received: 19 February 2009
Revised: 23 July 2009
Accepted: 27 July 2009
Published online: 29 August 2009
© European Society of Radiology 2009

D. G. H. Devos (✉)
Department Radiology–MRI (-1K12),
Ghent University Hospital,
De Pintelaan 185,
B-9000 Gent, Belgium
e-mail: Daniel.devos@uzgent.be
Tel.: +32-9-3324072
Fax: +32-9-3324969

P. J. Kilner
Department of Cardiac MRI,
Royal Brompton Hospital,
Sydney St,
London, SW3 6NP, UK

Abstract Background: Cardiovascular magnetic resonance measurements of the volumes of the right and left ventricle and of the flows in the ascending aorta and main pulmonary artery contribute to the assessment of patients with valvular regurgitation or intracardiac or extracardiac shunts. Ventricular volumes are measured by planimetry and summation of end-diastolic and end-systolic areas measured in a stack of ventricular short-axis cines. The volumes of blood flowing through planes transecting the great arteries are measured using phase contrast velocity mapping. The two approaches are essentially different and can be used either for mutual validation, or separately or in combination to quantify regurgitation and/or shunting. In the presence of shunts, the relations between the stroke volumes and arterial flows of each side of the heart vary depending on the level of shunting (for example, atrial, ventricular or ductal). **Conclusion:** This article aims to explain and

illustrate the technical and theoretical basis for calculations using volumetric and flow measurements, providing formulae and diagrams to facilitate the interpretation of results.

Keywords MRI · Flow velocity · Stroke volume · Quantification · Shunt

Abbreviations CMR: cardiovascular magnetic resonance · LV: left ventricle · RV: right ventricle · SV: stroke volume · V: volume · EDV: end diastolic volume · ESV: end systolic volume · Ao: ascending aorta · MPA: main pulmonary artery · R-R interval: interval between two successive R peaks of the electrocardiogram · RA: right atrium · Q_{Ao} : ascending aortic flow volume (per beat) · Q_{MPA} : pulmonary flow volume (per beat) · Q_P : pulmonary flow volume (per beat) · Q_S : systemic flow volume (per beat) · VENC: velocity encoding range

Introduction

Cardiovascular magnetic resonance (CMR), which has the advantages of freedom from ionizing radiation and unrestricted anatomical access, is a uniquely versatile modality for the evaluation of congenital and valvular heart disease in adults. Visualisation of cardiovascular morphology and connections is complemented by volumetric measurements of both ventricles, without geometric assumptions, and by measurements of the volumes of flow through large

vessels. Blood flow is measured using phase contrast velocity mapping through planes transecting the great arteries, which allows calculation of the volumes of forward flow and of diastolic regurgitation. Contrast-enhanced magnetic resonance angiography also allows the visualisation of vascular connections and branches, if required, and late gadolinium enhancement studies can be used to study scarring and viability of the myocardium [1–3]. This paper concentrates on the interpretation of CMR volumetric and flow measurements. The accuracy of such

measurements depends on the methods of acquisition and analysis used, and basic information on these is given. However, our main aim is to explain and illustrate the rational basis for the interpretation of such measurements, assuming appropriate methods of acquisition and post-processing to have been used.

Techniques

Ventricular volume measurements

Steady-state free precession (SSFP) cine images are well suited for volumetric analysis [4]. Normal values for left [5] and right [6] ventricular volume are published elsewhere. From transaxial multislice scout images, a left ventricular (LV) vertical long-axis cine is aligned, and a horizontal long-axis acquired orthogonal to it. In relation to these, a stack of ventricular short axis cines is aligned, covering the volumes of both ventricles from base to apex. Oblique four-chamber and three-chamber cines can also be aligned relative to these if required. The short-axis stack is typically acquired at 10-mm intervals, for example, as 6-mm slices with 4-mm gaps. SSFP sequences give excellent contrast between myocardium and blood, independent of the direction of inflow. With the use of retrospective ECG gating, cine frames are acquired throughout the cardiac cycle, including late diastole, as long as the cardiac rhythm is regular. For ventricular volume measurement, it is important to position the most basal short axis slice so that the most basal part of both right and left ventricles is just included in the slice at end diastole. Long-axis displacements of the left and right atrio-ventricular junctions during systole mean that the basal slice includes ventricular blood volume at end diastole but not necessarily at end systole. Long axis displacement of the base of the RV is normally greater than that of the LV, but both have to be accounted for during ventricular volume analysis, either by manual endoluminal contour delineation or by automated contour delineation; cross-sectional correlation with long-axis cine imaging helps to accurately define the position of the valve planes relative to the shortaxis images.

Endocardial borders of the free wall and apical regions of the right ventricle are normally highly trabeculated. This becomes even more apparent if the RV is hypertrophied [7]. For biventricular volume measurement, the correct phases must be chosen for the end-diastolic and end-systolic measurements. RV systole can continue slightly longer than LV systole, particularly in a volume or pressure loaded RV. The endocardial borders of most regions of the LV are also trabeculated, with trabeculations of the apical third merging into the papillary muscles in the mid third [8]. Most approaches to volumetric analysis trace simplified 'endocardial' contours just within the compact myocardial layers of each ventricle. This means that most trabeculations and the papillary muscles then lie within the

calculated blood volume. Inclusion versus exclusion of normal papillary muscles and trabeculations makes a difference in the order of magnitude of 6–8% [9]. Particularly in the presence of hypertrophy, the blood spaces between trabeculations become obliterated at end systole, obscuring the boundary between compact and trabeculated myocardium. An alternative approach to volumetric analysis, which uses semi-automated signal threshold analysis, appropriately counts all visible trabeculations and papillary muscles as myocardium [10]. This approach yields slightly smaller and arguably more accurate, but not necessarily more reproducible measurements of intraventricular blood volume than the simplified, peri-trabecular method of delineation.

Whichever method is used, consistency of analysis should be maintained in a particular centre if serial measurements of ventricular volume are to be compared. Appropriate training and practice are needed to achieve internally consistent volumetric measurements (see section on validation, below). For serial comparison, it is advisable to archive not only the image datasets, but also the boundaries traced during volume calculations for future reference.

Phase contrast velocity mapping

Phase contrast mapping of velocities through planes transecting the great arteries can potentially provide the most accurate in vivo measurements available of cardiac output, shunt flow and aortic or pulmonary regurgitation [11]. For such measurements, velocity is encoded through the plane of the image, in the direction of the slice select gradient. The image plane is oriented perpendicular to the direction of flow, transecting the axis of the tubular part of the aorta or main pulmonary artery (MPA) immediately above each sino-tubular junction at end diastole. While each velocity acquisition takes only a single breath hold, preparatory cine images aligned with each great artery are needed for correct location. Two cine images, perpendicular to each other but aligned with the centre axis of the vessel in which the flow is to be measured, serve as a basis for correct perpendicular positioning of the through-plane velocity encoded acquisition (Fig. 2). Preliminary acquisition of an in-plane encoded velocity map can help to define the direction of the flow and the velocity encoding range needed.

However, even when appropriate methods of acquisition have been used, there may still be inaccuracies of flow measurement on some CMR systems caused by background phase errors due to eddy currents or uncorrected concomitant gradients [12]. Measurements of regurgitant or shunt flow are particularly sensitive to such errors, which should be minimised or corrected by appropriate hardware and software design. If they have not been, inaccuracies can be detected and corrected by repeating

identical velocity acquisitions on a static phantom, and subtracting the corresponding apparent phantom velocities from those of the clinical acquisition [13]. In addition, aortic regurgitant volume may be underestimated due to the upward movement of the aortic root in diastole at the time when the regurgitant jet is flowing back into the ventricle. If the aortic root is dilated and mobile, the underestimation of the regurgitant fraction could be as much as 10 or 15% of the forward flow volume. A solution to this source of inaccuracy is the implementation of motion tracking and heart motion adapted flow measurements as described by Kozerke and colleagues in 1999 and 2000 [14, 15]. However, the technique has yet to be made available on most commercial CMR systems.

As with Doppler flow measurement, velocity information encoded in phase shifts is subject to aliasing. To avoid aliasing, an appropriate velocity encoding range (VENC) should be chosen before acquiring velocity data. An appropriate VENC exceeds the peak expected velocity by 10–50%. Too high a VENC reduces the sensitivity of velocity mapping by reducing the amount of velocity-related phase shifts relative to background noise or other artefact-related phase shifts.

Grading of regurgitation lesions by ultrasound is a combination of qualitative and quantitative assessment. In CMR the morphology of a regurgitant or stenotic jet should not be used to grade a lesion, because not only lesion characteristics but also sequence parameters influence jet morphology. Quantification of peak velocity, regurgitant volume and fraction, as well as jet area (analogous to orifice area) in CMR provide the most accurate methods for valve lesion evaluation [12]. Valve lesion grading by CMR has been compared with ultrasound for aortic stenosis [16], aortic regurgitation [17, 18], mitral regurgitation [18] and pulmonary regurgitation after tetralogy of Fallot (where CMR was used as the gold standard) [19]. Correlation of grading was good to very good. Specific cutoff values for CMR grading of valve lesions have not been defined, but provisional values based on a combination of our own experience and previous echocardiographic guidelines [20–22] are suggested in Table 1.

Validation techniques

There is no gold standard with which to correlate the CMR measurement of ventricular volume [23]. It is difficult to compare CMR measured in vivo volumes with post-mortem measurements because of changed characteristics of the post-mortem myocardium. Although comparisons are possible with volume measurements by other imaging techniques, most alternatives are likely to be less precise as they are based on assumptions about the geometry of the ventricle, or, in the case of multidetector computed tomography, dependent on adequate opacification of both ventricular cavities.

However, the two sides of the heart function in series with one another and, in the absence of shunts or regurgitation, the left and right ventricles should have equal stroke volumes (SV) and similar outputs. Cross validation is therefore possible in healthy volunteers and in patients who can be shown to have neither shunting nor regurgitation. RVSV should then be equal to LVSV, and each of these should be equal to the aortic or pulmonary outflow per beat. In the following, we will represent the net aortic and main pulmonary artery forward flow per beat as Q_{Ao} and Q_{MPA} , respectively. In most but not all cases, these can be taken as being the same systemic flow (Q_p) and pulmonary flow (Q_s) per beat. The most commonly encountered exception is where there is a patent ductus arteriosus (PDA) shunting from the systemic to pulmonary arterial side, distal to the planes of flow measurement.

Clinical application

In this section, formulae for clinically relevant calculations of regurgitant or shunt lesions from volume and flow measurements are given. Abbreviations used are defined at the beginning of the article. The stroke volumes are measured from planimetry of the short axis cine acquisitions. The flow volumes are measured velocity maps.

Normal, and heart disease without shunting or regurgitation

$$LVSV = RVSV = Q_{Ao} = Q_{MPA} \quad (1)$$

The stroke volumes of the left and right ventricles should be the same, and each of these should be the same as the net forward flow per beat in the ascending aorta or the main pulmonary artery (Q_{Ao} or Q_{MPA} , respectively), with the relatively minor proviso that coronary flow, which may be about 5% of the ejected volume, is not included in aortic flow if it is measured just distal to the sino-tubular junction. A schematic diagram of a normal heart is shown in Fig. 1a. The diagrams do not attempt to represent the venous structures.

Mitral regurgitation

$$LVSV - \text{mitral regurgitant volume} = Q_{Ao} = RVSV = Q_{MPA} \quad (2)$$

$$\text{mitral regurgitant volume} = LVSV - RVSV = LVSV - Q_{Ao} \quad (3)$$

$$\text{regurgitant fraction in \%} = \text{regurgitant volume} \times 100 \div LVSV \quad (4)$$

Table 1 A provisional guide to the severity of regurgitant heart valve disease in adults as assessed by CMR, based on a combination of the authors' experience and the ranges published in the 2006 ACC/AHA guidelines on the management of valvular heart disease, the latter of which are based mainly on echocardiographic indices [20–22]. Orifice area and stream width values in the lower range should be regarded as estimations rather than accurate measurements, given the limits of spatial resolution of the CMR images

Aortic regurgitation			
	Mild	Moderate	Severe
Regurgitant volume (ml per beat)	<30	30–60	>60 (body size is relevant, but indexed values are not available)
Regurgitant fraction	<30%	30–50%	>50% (CMR flow measurements tend to underestimate AR, unless corrected for aortic root motion)
Regurgitant orifice area (cm ²)	<0.1	0.1–0.3	>0.3
Pulmonary regurgitation (assuming near normal pulmonary resistance)			
	Mild	Moderate	“Free” or “almost free” (but may be well tolerated)
Regurgitant jet or stream width	Narrow, <2 mm	Moderate 2–5 mm	Unobstructed reversed stream, >6 mm across
Valve leaflet appearances	Mobile, coapting	Partly coapting	Ineffective leaflets with wide failure of coaptation.
Regurgitant volume (ml per beat)	<30	30–40	>40 (body size is relevant, but indexed values are not available)
Regurgitant fraction	<25%	20–35%	>35%, but modified by up- and downstream factors
Additional features			Free PR occurs mainly in the first half of diastole, typically followed by late diastolic forward flow, if the right ventricle has been fully distended by the onset of atrial systole
Mitral regurgitation			
	Mild	Moderate	Severe
Regurgitant jet width	Narrow, <1.0 mm	1.0–2 mm	>2 mm, with extensive jet or swirling flow in left atrium
	No visible jet core	Narrow jet core	Bright jet core >2 mm in width (if cine is suitably located)
Regurgitant volume (ml per beat)	<30	30–60	>60 (body size is relevant, but indexed values are not available)
Regurgitant fraction	<30%	30–50%	>50%
Regurgitant orifice area (cm ²)	<0.2	0.2–0.4	>0.4
Additional features			Dilated left atrium and pulmonary veins Systolic flow reversal in pulmonary veins
Tricuspid regurgitation (assuming near normal pulmonary resistance)			
	Mild	Moderate	Severe
Regurgitant fraction	<30%	30—about 40%	(Regurgitant fraction unreliable due to measurement difficulties and conduit-like function of a distended right heart)
Regurgitant jet width	Narrow, <2 mm	2–6 mm	>6×6 mm, measured on a through plane velocity map
Additional features			Dilated right atrium and caval veins

In isolated mitral insufficiency (Fig. 1b), the contracting LV ejects blood back to the left atrium as well as forward to the aorta, resulting in volume loading of the left side of the heart. Aortic and pulmonary velocity mapping should not show a difference in ejected blood volumes. Q_{Ao} or Q_P may be subtracted from the LVSF to calculate the mitral regurgitant volume, or either may be used to cross check the RVSF measurement [18, 24].

It will be apparent that the calculation of mitral regurgitation from CMR is indirect, depending on at least three sets of measurements (LVEDV, LVESV and Q_{Ao} , or else LVEDV, LVESV, RVEDV and RVESV). For this reason, rigorous methods of acquisition and measurement are needed, and even if used, there may still be scope for error. It is therefore recommended that CMR quantification of mitral regurgitation is complemented by cine imaging of

all parts of the valve with a contiguous stack of appropriately orientated long-axis cines, and in the case of ischaemic mitral regurgitation, by late gadolinium assessment of the left ventricular scar and viability [3].

Direct mapping of regurgitant flow through the mitral valve cannot yet be recommended as it may be prone to error due to turbulence of the high velocity jet, the movement of the valve plane during systole and the possible entrainment of intra-atrial blood by the regurgitant jet.

Tricuspid regurgitation

$$\begin{aligned} \text{RVSV} - \text{tricuspid regurgitant volume} &= Q_{\text{MPA}} \\ &= \text{LVSV} = Q_{\text{Ao}} \end{aligned} \quad (5)$$

$$\begin{aligned} \text{tricuspid regurgitant volume} \\ &= \text{RVSV} - \text{LVSV}, \text{ or } \text{RVSV} - Q_{\text{MPA}} \end{aligned} \quad (6)$$

$$\begin{aligned} \text{regurgitant fraction in \%} \\ &= \text{regurgitant volume} \times 100 \div \text{RVSV} \end{aligned} \quad (7)$$

The formulae given are comparable to those for mitral regurgitation. However, severely regurgitant lesions of the right heart may not be directly comparable to those of the left. A grossly dysfunctional right heart can function transiently as a conduit, with its inflow and outflow valves open simultaneously, the forward flow being maintained indirectly by work of the left heart. If this is the case, relative volumetric measurements may not be so informative. Furthermore, increased amplitude of long-axis movement of the base of the RV may make accurate volumetric measurement challenging. For these reasons, thorough cine imaging of the valve, for example using a contiguous stack of transaxial cines, is recommended, followed by through-plane velocity mapping of the regurgitant jet immediately on the atrial side of the valve. We do not rely on this velocity acquisition for volumetric calculation, which may be subject to the errors listed in the previous section, but rather for delineation of the cross-sectional area of the jet. If this velocity acquisition provides clear delineation, we believe that this reflects the size, shape and hence severity of the tricuspid regurgitant orifice, although data in support of this have yet to be published.

Aortic and pulmonary regurgitation (Fig. 1c)

$$\begin{aligned} \text{Regurgitant volume} &= \text{diastolic reversed flow volume} \\ & \quad (8) \end{aligned}$$

$$\begin{aligned} (\text{isolated}) \text{ aortic regurgitant volume} &= \text{LVSV} - \text{RVSV} \\ & \quad (9) \end{aligned}$$

Fig. 1 A schematic diagram is shown, with indication of blood displacement, of a normal heart (a), an MR (b), an AR (c), an ASD (d), a VSD (e), a PDA (f), a Gerbode defect (g), an extracardiac systemic arterial-to-venous shunt (h) and an Eisenmenger complex (i). The venous structures are not drawn for clarity

Aortic regurgitant fraction (%) = diastolic reversed

$$\begin{aligned} &\text{flow volume} \times 100 \div \text{systolic forward flow volume} \\ & \quad (10) \end{aligned}$$

Ascending aortic and MPA velocity maps themselves provide relatively direct data for calculations of the regurgitant volume (or regurgitant fraction) of the outflow valves. Most phase contrast analysis software packages calculate forward and reversed flow volumes, and from them, the regurgitant fraction. However, it should be borne in mind that the regurgitant volume calculated is highly sensitive to possible uncorrected phase offset errors (see phase velocity mapping section, above), especially if the vessel studied is dilated. Chatzimavroudis et al. have measured that with increasing slice distance from the aortic valve, a decrease in measured regurgitant volume occurs due to an aortic compliance effect [25].

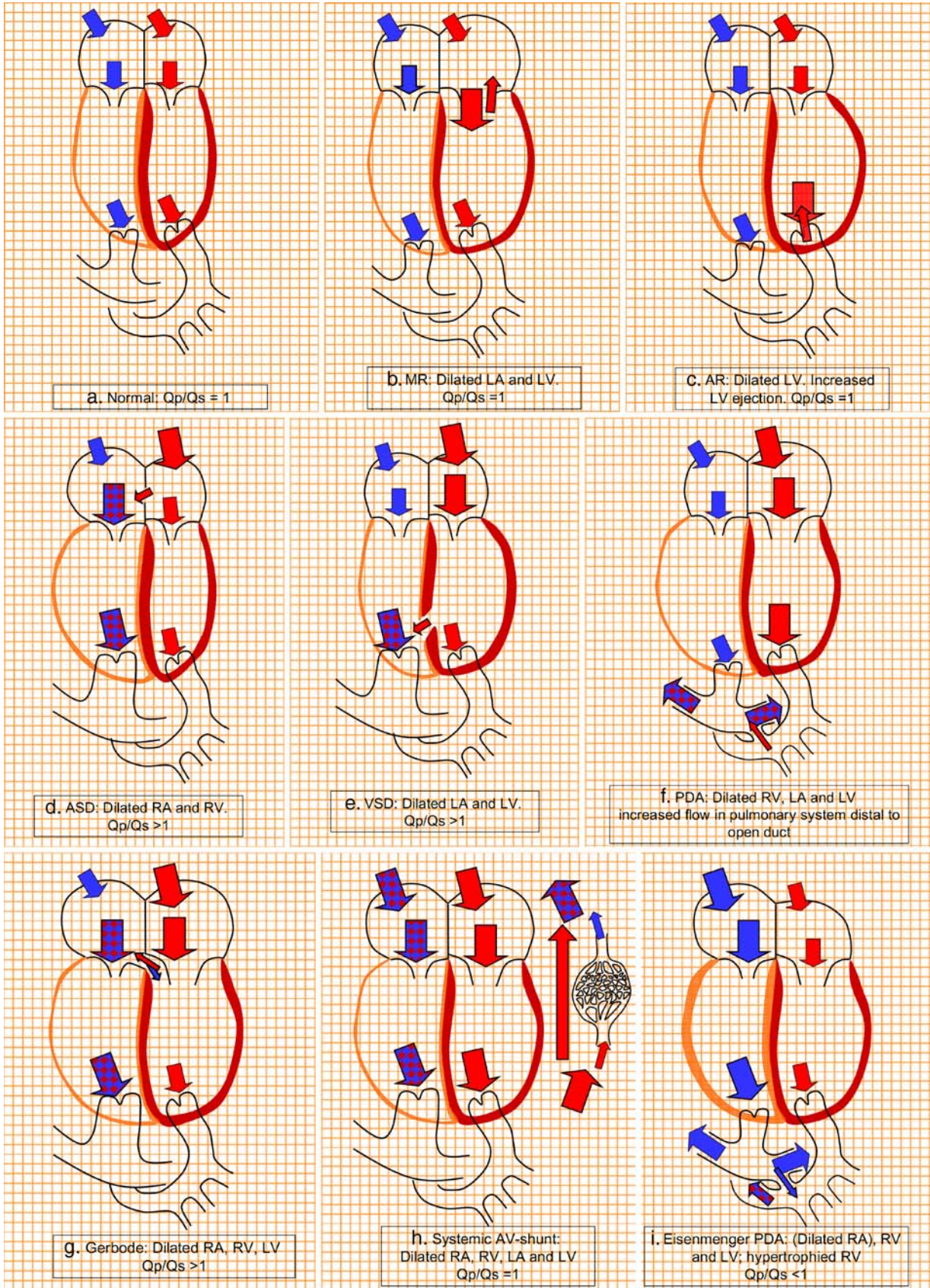
Free or nearly free pulmonary regurgitation (PR) is not directly comparable with severe aortic regurgitation. Free PR, which is relatively common after repair of tetralogy of Fallot, may be tolerated for decades, and is usually associated with a regurgitant fraction of about 40%. This should not necessarily be regarded as ‘severe’. A regurgitant fraction of 50% or more, which would correctly be regarded as severe, is unusual, and may be attributable to additional factors such as distal PA branch stenosis or elevated pulmonary resistance. Wald et al. have argued that indexed pulmonary regurgitant volume may be preferable to regurgitant fraction [26], but further research is needed to establish criteria for severity by this approach.

If only one valve is regurgitant, the difference between RV and LV stroke volumes should give the regurgitant volume, but this calculation depends on four sets of tracings and measurements and may be of questionable accuracy. Volumetric measurements mostly contribute to evaluation of effects of the volume load on the respective ventricle.

Atrial septal defect

$$\begin{aligned} \text{RVSV} &= \text{LVSV} + \text{ASD Shunt volume} = Q_{\text{MPA}} \\ & \quad = Q_{\text{Ao}} + \text{ASD shunt volume} \end{aligned} \quad (11)$$

Atrial septal defect (ASD) (Fig. 1d) is the commonest cause of intracardiac shunting. The shunting is typically



mainly from left to right as pressure tends to be higher in the left atrium than the right. This results in volume loading and dilatation of the right ventricle and the pulmonary arteries. The RV stroke volume, which delivers Q_{MPA} , returns from the lungs to the left atrium where it delivers both the volume shunted across the ASD and volume flowing forward to the LV, which is then ejected as Q_{Ao} .

An ostium secundum ASD may be visible in an atrial short-axis cine stack, scanned parallel to the ventricular short axis, but covering all atrial regions. Through-plane velocity mapping aligned parallel to the septum, thus transecting the left to right stream of ASD flow, with the VENC set at 1 m/s, can be useful for visualising and delineating the defect(s).

An ostium secundum ASD of about 10–20 mm in diameter typically results in a pulmonary-systemic flow ratio ($Q_P:Q_S$) of between 1.5 and 2.5:1.0. The ratio may be modified, however, by valvular or ventricular disease on either side, or by the development of pulmonary arterial hypertension.

Partial anomalous pulmonary venous drainage is frequently associated with a superior sinus venosus ASD (Fig. 2), which should be visible in a contiguous stack of transaxial cine images, apparent as absence of the uppermost part of the atrial septum, immediately beneath the SVC. If a full stack of transaxial mediastinal cines are acquired, they also allow identification of anomalous pulmonary venous drainage. This can be confirmed and displayed in 3D using contrast-enhanced CMR angiography. The commonest anomaly is a right upper pulmonary vein draining to the superior vena cava. This adds to the amount of 'left' to 'right' shunting. In our experience, a sinus venosus ASD with a pulmonary vein draining to the SVC is typically associated with a large pulmonary/systemic flow ratio ($Q_P:Q_S$), i.e., at least 2.5:1.0. Shunt volumes of any partial anomalous pulmonary venous connection should be measured in the same way as an ASD (Fig. 3).

Ventricular septal defect

$$\begin{aligned} LVS\!V &= RVS\!V + \text{VSD shunt volume} = Q_{MPA} \\ &= Q_{Ao} + \text{VSD shunt volume} \end{aligned} \quad (12)$$

A ventricular septal defect (VSD) (Fig. 1e) allows flow of blood between the LV and the RV. As pressure is usually higher in the LV, blood shunts from left to right, mainly during systole and less, if at all, during diastole. The shunt is associated with volume loading of the left but not the right ventricle. It is, however, associated with increased pulmonary relative to aortic blood flow. This

Fig. 2 A 46-year-old man with suspected sinus venosus ASD. MR for evaluation of shunt and pulmonary venous return. Volume measurement (not shown) resulted in $RVS\!V=193$ ml and $LVS\!V=108$ ml. Flow-mapping in the positions indicated by a yellow straight line resulted in stroke volumes: (a, b, c) for aorta, $Q_{Ao}=102$ ml; (d, e, f) for pulmonary trunk, $Q_{MPA}=221$ ml; (g, h, i) direct measurement in ASD=121 ml. Angiographic image (j) in orientation comparable to (g) shows pulmonary vein entering SVC and SVC overriding the atrial septum; curved arrow indicates sinus venosus ASD. Still image from cine loop in oblique four-chamber view (k) shows sinus venosus ASD (curved arrow) $Q_P/Q_S = 2/1$

may seem paradoxical, but it is explained by the VSD shunt volume passing in and out of the contracting right ventricle without having added to the RV end diastolic volume.

With experience, a VSD can usually be identified on routine CMR cine acquisitions by the appearance of systolic jet flow on the RV side of the septum. Such jet flow is most commonly seen in one of the more basal short axis slices that pass through the region of the membranous septum.

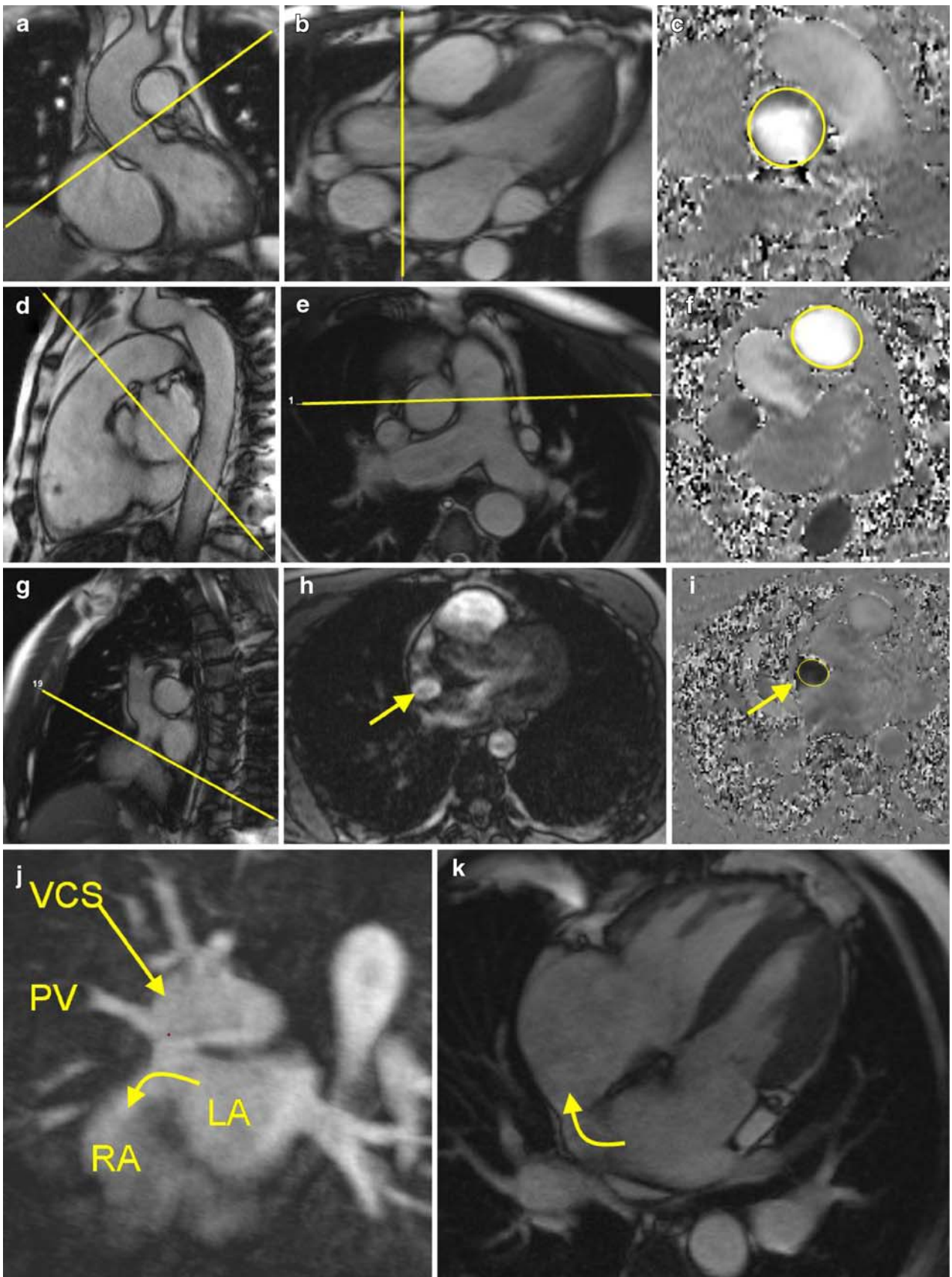
A large non-restrictive VSD can be associated with so much left to right shunting that pulmonary vascular disease and pulmonary hypertension result. When systolic PA pressure exceeds systemic pressure, a net right-to-left shunting across the VSD occurs, known as an Eisenmenger VSD, with resulting cyanosis.

Patent ductus arteriosus

$$\begin{aligned} LVS\!V &= Q_{Ao} = RVS\!V + \text{PDA shunt volume} \\ &= Q_{MPA} + \text{PDA shunt volume} \\ &= Q_P = Q_S + \text{PDA shunt volume} \end{aligned} \quad (13)$$

A patent ductus arteriosus (PDA) (Fig. 1f) allows blood flow between the descending aortic arch and the bifurcation of the MPA. If the duct is relatively small, it typically results in continuous jet flow directed anteriorly into the uppermost part of the MPA. Detection of a PDA by CMR is initially based on the detection of a jet on cine imaging or by 3D depiction of the duct by contrast-enhanced CMR angiography.

A PDA generally causes left ventricular volume loading and dilatation of the LV, with increased flow to the distal pulmonary artery branches. However, it is important to realize that the PDA shunt occurs distal to the planes of Q_{Ao} and Q_{MPA} measurement, so there is usually higher flow in the ascending aorta than in the pulmonary trunk. Therefore, the Q_{MPA}/Q_A ratio is usually



the inverse of the Q_p/Q_s ratio. The exception to this is when a large ‘Eisenmenger’ PDA is associated with pulmonary arterial hypertension and net pulmonary-aortic shunting.

Gerbode defect

$$LVSV = Q_{A_0} + \text{gerbode shunt volume} = RVSV = Q_{MPA} \quad (14)$$

The tricuspid valve is positioned slightly more apically than the mitral valve. Therefore, it is normal for part of the LV to lie adjacent to the right atrium (RA), separated from the RA by a small part of the membranous ventricular septum. A congenital defect of this LV/RA septum is known as a Gerbode defect (Fig. 1g). In 1958, Gerbode was the first to describe surgical correction in five cases thought to have been congenital in origin [27]. Comparable defects can also be acquired, after previous aortic root surgery, endocarditis, trauma or myocardial infarction. Most Gerbode defects are small, and diagnosis may be delayed. With transthoracic ultrasound the systolic jet is easily mistaken for a tricuspid insufficiency jet. A Gerbode defect volume loads both the RV and the LV, causing both ventricles to dilate, but Q_{MPA} will be larger than Q_{A_0} by the volume of the shunt.

However, if the defect is large it may lead to elevated RV filling pressure so that part of the shunted volume is returned to the LV in diastole rather than passing on to the RV, effectively adding to the LV stroke volume.

Extracardiac arterio-venous shunt

$$LVSV = Q_{A_0} = RVSV = Q_{MPA} \quad (\text{but all may be elevated}) \quad (15)$$

A shunt connecting arterial to venous branches of the systemic circulation (Fig. 1h), with local absence of high resistance microvessels, allows increased cardiac output. RV and LV stroke volumes should remain equal but increased. Q_{A_0} and Q_{MPA} , measured proximal to the abnormal vessels, should also be equal but increased. The same principle applies to most surgically constructed systemic-arterial shunts such as a Blalock-Taussig shunt, except that the shunt may have been placed in a patient who also had an unrepaired intracardiac shunt.

RV and LV stroke volumes should also remain equal if there is a pulmonary arterio-venous malformation,

although this may have less effect on cardiac output than a systemic shunt.

Eisenmenger syndrome

Eisenmenger (Fig. 1i) is the end-stage situation of a left to right inter-ventricular or inter-arterial shunt where the increased pulmonary blood flow has led to pulmonary vascular disease to such a degree that pulmonary arterial pressures exceed aortic. The net shunting then reverses, with flow of deoxygenated blood into the systemic arteries causing cyanosis. Quantification of such a shunt depends on the underlying defect. The high resistance to flow through the lungs tends to result in reduced venous return to the left heart, and abnormally low stroke volume and output. Thrombo-embolic disease, or the development of mural thrombus in the dilated and sluggishly flowing pulmonary arteries, is relatively common in such patients, and may be identified using contrast-enhanced pulmonary angiography.

Conclusion

This paper provides descriptions, formulae and illustrations to support calculations from CMR volumetric and flow measurements of regurgitant or shunt flow. CMR is extremely versatile, and through-plane phase contrast velocity mapping potentially provides the most accurate measurements available of regurgitant or shunt flow, as long as potential errors are avoided, or recognised and corrected. Table 2 provides an overview of the changes in stroke volume from cine volumetry and ventricular outflow as measured by phase contrast imaging per pathology.

We have not attempted to address the numerous possible combinations of lesions. However, if the principles are understood and the circulatory abnormalities of a particular case are thought through carefully, it is usually possible to calculate the amount of shunting or regurgitation in the presence of additional lesions. Occasionally, it may be helpful to make measurements of flow-through planes transecting additional vessels, for example, the caval veins or the right and left pulmonary arteries. However, it should be borne in mind that more complex calculations give greater scope for cumulative error. In general, the simpler the calculation, the better.

In all cases it is advisable to acquire complementary visual evidence of the dimensions and nature of the regurgitant or shunt flow being measured. In the majority, this will be jet flow, which can be well visualised on appropriately aligned

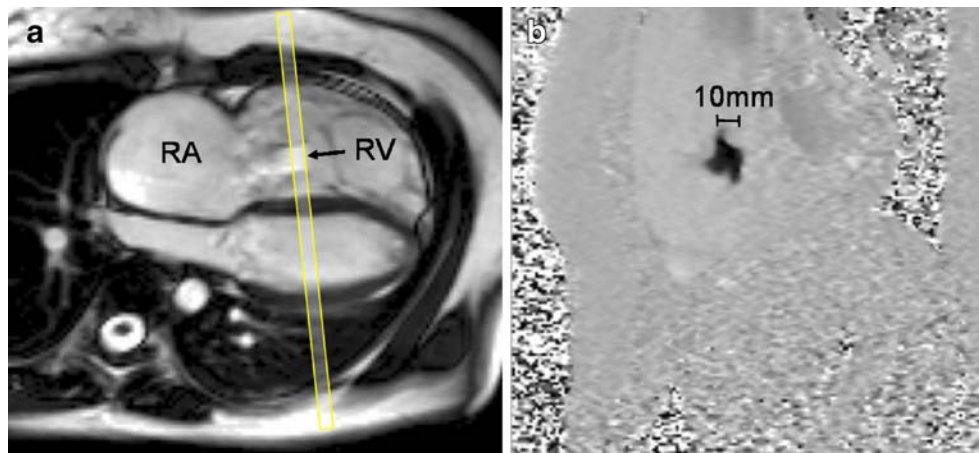


Fig. 3 Severe tricuspid regurgitation. A systolic frame of a four-chamber cine acquisition aligned with the centres of the inflow valves (panel **a**.) shows a dilated right atrium (RA) and right ventricle (RV) with evidence of a broad tricuspid regurgitant stream (arrow). The bar indicates the location of a through-plane velocity

acquisition (panel **b**), VENC set at 250 cm/s. In this case, the well-defined dark flow area confirms a broad, severely regurgitant stream, over 10 mm across. In the absence of any shunt, this is associated with an elevated RV stroke volume relative to that of the left ventricle, but equal pulmonary and aortic flow volumes

SSFP cine images, or stacks of cine images. In SSFP images, the shear layers on either side of a jet appear relatively dark because of signal dephasing. The core of the jet can appear relatively bright, as long as it is broad and coherent enough, and appropriately aligned to contain whole voxels. In the case of broad, relatively low velocity streams, for example, through an ASD or a severely regurgitant tricuspid or pulmonary valve, bounding shear layers may not be clearly apparent. If so, mapping of velocities with appropriately low VENC through a plane transecting the (regurgitant) stream immediately ‘downstream’ of its orifice can depict its cross

section, which gives a useful guide to the cross-sectional area of the orifice.

Quantitative calculations depend on the quality and expected accuracy of acquisitions and post processing. Rigorous methods should be maintained, and validation practiced periodically, either using the intra-study cross checks outlined above, or using subsequent phantom correction of suspected flow offset errors [13]. If doubt remains in a particular clinical case, measurements made should either not be reported, or qualified by a phrase such as ‘of questionable accuracy’.

Table 2 Overview of the changes in stroke volume from cine volumetry and ventricular outflow as measured by phase contrast imaging per pathology

Defect	Shunt	RVSV	LVSV	Q_{MPA}	Q_{Ao}
Mitral regurgitation	None		Increased		
Tricuspid regurgitation	None	Increased			
ASD	LA → RA	Increased		Increased	
VSD	LV → RV		Increased	Increased	
PDA	Ao arch → distal MPA		Increased		Increased
Gerbode defect	LV → RA	Increased	Increased	Increased	
Systemic artery→vein shunt	Artery → vein	Increased	Increased	Increased	Increased
Eisenmenger VSD	RV → LV		Decreased	Decreased	
Eisenmenger PDA	Distal MPA → Ao arch		Decreased		Decreased

References

- Nigri M, Azevedo CF, Rochitte CE, Schraibman V, Tarasoutchi F, Pommerantzeff PM, Brandão CM, Sampaio RO, Parga JR, Avila LF, Spina GS, Grinberg M (2009) Contrast-enhanced magnetic resonance imaging identifies focal regions of intramyocardial fibrosis in patients with severe aortic valve disease: correlation with quantitative histopathology. *Am Heart J* 157:361–368
- Isbell DC, Kramer CM (2006) Magnetic resonance for the assessment of myocardial viability. *Curr Opin Cardiol* 21:469–472
- Chan KMJ, Wage R, Symmonds K, Rahman-Haley S, Mohiaddin R, Firmin DN, Pepper J, Pennell DJ, Kilner PJ (2008) Towards comprehensive assessment of mitral regurgitation using cardiovascular magnetic resonance. *J Cardiovasc Magn Res* 10:61–72
- Carr JC, Simonetti O, Bundy J, Li D, Pereles S, Finn JP (2001) Cine MR angiography of the heart with segmented true fast imaging with steady-state precession. *Radiol* 219:828–834
- Maceira A, Prasad S, Khan M, Pennell D (2006) Normalized left ventricular systolic and diastolic function by steady state free precession cardiovascular magnetic resonance. *J Cardiovasc Magn Res* 8:417–426
- Maceira AM, Prasad SK, Khan M, Pennell DJ (1-12-2006) Reference right ventricular systolic and diastolic function normalized to age, gender and body surface area from steady-state free precession cardiovascular magnetic resonance. *Eur Heart J* 27:2879–2888
- Winter M, Bernink F, Groenink M, Bouma B, van Dijk A, Helbing W, Tijssen J, Mulder B (2008) Evaluating the systemic right ventricle by CMR: the importance of consistent and reproducible delineation of the cavity. *J Cardiovasc Magn Res* 10:40
- Axel L (2004) Papillary muscles do not attach directly to the solid heart wall. *Circ* 109:3145–3148
- Ibrahim T (1999) Effect of papillary muscles and trabeculae on left ventricular parameters in cinemagnetic resonance images. *Journal of Cardiovascular Magnetic Resonance* 1:319–319
- Codella NCF, Weinsaft JW, Cham MD, Janik M, Prince MR, Wang Y (2008) Left ventricle: automated segmentation by using myocardial effusion threshold reduction and intravoxel computation at MR imaging. *Radiol* 248:1004–1012
- Gatehouse P, Keegan J, Crowe L, Masood S, Mohiaddin R, Kreitner KF, Firmin D (2005) Applications of phase-contrast flow and velocity imaging in cardiovascular MRI. *Eur Radiol* 15:2172–2184
- Kilner PJ, Gatehouse PD, Firmin DN (2007) Flow measurement by magnetic resonance: a unique asset worth optimising. *J Cardiovasc Magn Res* 9:723–728
- Chernobelsky A, Shubayev O, Comeau CR, Wolff SD (2007) Baseline correction of phase contrast images improves quantification of blood flow in the great vessels. *J Cardiovasc Magn Res* 9:681–685
- Sebastian K, Juerg Schwitler E (2001) Aortic and mitral regurgitation: quantification using moving slice velocity mapping. *J Magn Reson Imaging* 14:106–112
- Sebastian K, Markus BS (1999) Heart motion adapted cine phase-contrast flow measurements through the aortic valve. *Magn Reson Med* 42:970–978
- Caruthers SD, Lin SJ, Brown P, Watkins MP, Williams TA, Lehr KA, Wickline SA (4-11-2003) Practical value of cardiac magnetic resonance imaging for clinical quantification of aortic valve stenosis: comparison with echocardiography. *Circ* 108:2236–2243
- Wittlinger T, Dzemali O, Bakhtiary F, Moritz A, Kleine P (2008) Hemodynamic evaluation of aortic regurgitation by magnetic resonance imaging. *Asian Cardiovasc Thorac Ann* 16:278–283
- Gelfand EV (2006) Severity of mitral and aortic regurgitation as assessed by cardiovascular magnetic resonance: optimizing correlation with Doppler echocardiography. *J Cardiovasc Magn Res* 8:503–507
- Grothoff M, Spors B, bdul-Khaliq H, Gutberlet M (10-2-2008) Evaluation of postoperative pulmonary regurgitation after surgical repair of tetralogy of Fallot: comparison between Doppler echocardiography and MR velocity mapping. *Pediatr Radiol* 38:186–191
- Bonow RO, Carabello BA, Chatterjee K, de Leon AC Jr, Faxon DP, Freed MD, Gaasch WH, Lytle BW, Nishimura RA, O’Gara PT, O’Rourke RA, Otto CM, Shah PM, Shanewise JS (2006) ACC/AHA 2006 guidelines for the management of patients with valvular heart disease: a report of the American College of Cardiology/American Heart Association Task Force on practice guidelines (Writing Committee to Revise the 1998 guidelines for the management of patients with valvular heart disease): developed in collaboration with the Society of Cardiovascular Anesthesiologists: endorsed by the Society for Cardiovascular Angiography and Interventions and the Society of Thoracic Surgeons. *Circ* 114:e84–e231
- Bonow RO, Carabello BA, Chatterjee K, de Leon AC Jr, Faxon DP, Freed MD, Gaasch WH, Lytle BW, Nishimura RA, O’Gara PT, O’Rourke RA, Otto CM, Shah PM, Shanewise JS, Nishimura RA, Carabello BA, Faxon DP, Freed MD, Lytle BW, O’Gara PT, O’Rourke RA, Shah PM (2008) 2008 focused update incorporated into the ACC/AHA 2006 guidelines for the management of patients with valvular heart disease: a report of the American College of Cardiology/American Heart Association Task Force on practice guidelines (Writing Committee to Revise the 1998 guidelines for the management of patients with valvular heart disease) endorsed by the Society of Cardiovascular Anesthesiologists, Society for Cardiovascular Angiography and Interventions, and Society of Thoracic Surgeons. *J Am Coll Cardiol* 52:e1–e142
- Correction for Bonow et al. *Circulation* 114(5):e84–e231. (17-4-2007) *Circ* 115:e409- Available via: <http://circ.ahajournals.org/cgi/content/full/115/15/e409>, Accessed 18 June 2009
- Moon JCC, Lorenz CH, Francis JM, Smith GC, Pennell DJ (2002) Breath-hold FLASH and FISP cardiovascular MR imaging: left ventricular volume differences and reproducibility. *Radiol* 223:789–797

-
24. Kon MW, Myerson SG, Moat NE, Pennell D (2004) Quantification of regurgitant fraction in mitral regurgitation by cardiovascular magnetic resonance: comparison of techniques. *J Heart Valve Dis* 13:600–607
 25. Chatzimavroudis GP, Walker PG, Oshinski JN, Franch RH, Pettigrew RI, Yoganathan AP (1997) Slice location dependence of aortic regurgitation measurements with MR phase velocity mapping. *Magn Reson Med* 37:545–551
 26. Wald RM, Redington AN, Pereira A, Provost YL, Paul NS, Oechslin EN, Silversides CK (2009) Refining the assessment of pulmonary regurgitation in adults after tetralogy of Fallot repair: should we be measuring regurgitant fraction or regurgitant volume? *Eur Heart J* 30:356–361
 27. Gerbode F, Hultgren H, Melrose D, Osborn J (1958) Syndrome of left ventricular-right atrial shunt: successful surgical repair in five cases with observation of bradycardia on closure. *Ann Surg* 148:433–446